Solubilization of Carbon Nanofibers with a Covalently Attached Hyperbranched Poly(ether ketone)

David H. Wang,[†] Peter Mirau,[‡] Bing Li,[§] Christopher Y. Li,[§] Jong-Beom Baek,[△] and Loon-Seng Tan*,[‡]

University of Dayton Research Institute, Dayton, Ohio 45469-0168, Polymer Branch, AFRL/MLBP, Materials & Manufacturing Directorate, Air Force Research Laboratory, Wright-Patterson AFB, Ohio 45433-7750, Department of Materials Science and Engineering, Drexel University, Philadelphia, Pennsylvania 19104, and Department of Industrial Chemistry, Chungbuk National University, Chungbuk 361-763, South Korea

Received October 3, 2007. Revised Manuscript Received November 9, 2007

Because 5-phenoxyisophthalic acid, an A_2B monomer (where A denotes an acid functionality and B an activated aromatic C−H), was easily polymerized via a Friedel–Crafts acylation in poly(phosphoric acid)/phosphorus pentoxide [PPA/P_2O_5; 1:4 (w/w)] to form a CO_2H-terminated hyperbranched poly(ether ketone), HPB-PEK, it was polymerized in the presence of various amounts (1, 2, 5, 10, 20, 30, and 40 wt %) of vapor-grown carbon nanofibers (VGCNFs) under similar reaction conditions to form polymers grafted to VGCNFs. Considering the potential of cross-linking reactions during polycondensation processes because of the multifunctionality existing in each reacting species, it is remarkable that no gelation was observed for all of the in situ synthesis experiments conducted. The collective evidence based on the data from Soxhlet extraction (mass balance), elemental analysis, thermogravimetric analysis, Fourier-transform infrared spectroscopy, nuclear magnetic resonance, scanning electron microscopy, and transmission electron microscopy of the resulting materials implicates that, under our reaction conditions, most of the HPB-PEK (>93 wt % estimated) was grafted to the surfaces of VGCNFs, resulting in the formation of highly coated nanofibers. The grafted (HPB-PEK)-*g*-VGCNF materials were practically insoluble in dichlorobenzene or toluene but showed distinctly improved solubility in polar solvents such as *N*-methyl-2-pyrrolidone, *N*,*N*-dimethylformaide, dimethylacetamide, and ethanol and even higher solubility in a ethanol/triethylamine mixture or in a 10% aqueous ammonia solution, apparently promoted by the numerous peripheral CO_2H groups. From the intrinsic viscosity data analysis, all (HPB-PEK)-*g*-VGCNFs appeared to behave like an organic polymer in dilute solution and show rodlike character with increasingly shorter/smaller HPB-PEK grafts. As a way to determine both the ease in performing a chemical transformation on the periphery of the hyperbranched component of the resulting (HPB-PEK)-*g*-VGCNF and the end-group effect on some of their physical properties, the carboxylic acid end groups of the 10 wt % (HPB-PEK)-*g*-VGCNF were converted to benzothiazole, dodecyl ester, and amine end groups. As an example of how these transformations alter the physical properties, the dodecyl-terminated nanocomposite displayed an excellent solubility in chloroform and a much lower T_g than the CO_2H-terminated (HPB-PEK)-*g*-VGCNF.

Introduction

Carbon nanotubes (CNTs) including single-walled (SWNT) and multiwalled (MWNT) nanotubes[1] and, more recently, double-walled (DWNT)[2] and few-walled (FWNT) nanotubes[3] have sparked intense excitement in materials research

* To whom correspondence should be addressed. Tel: (937) 255-9141. Fax: (937) 255-9157. E-mail: loon-seng.tan@wpafb.af.mil.
[†] University of Dayton Research Institute.
[‡] Air Force Research Laboratory.
[§] Drexel University.
[△] Chungbuk National University.

(1) For some recent reviews on SWNT and MWNT, see: (i) Mahar, B.; Laslau, C.; Yip, R.; Sun, Y. *IEEE Sens. J.* **2007**, *7*, 266. (ii) Robertson, J. *Mater. Today (Oxford, U.K.)* **2007**, *10* (1–2), 36. (iii) Campidelli, S.; Klumpp, C.; Bianco, A.; Guldi, D. M.; Prato, M. *J. Phys. Org. Chem.* **2006**, *19*, 531. (iv) See, C. H.; Harris, A. T. *Ind. Eng. Chem. Res.* **2007**, *46*, 997. (v) Nakashima, N. *Sci. Technol. Adv. Mater.* **2006**, *7*, 609. (vi) Avouris, P.; Chen, J. *Mater. Today (Oxford, U.K.)* **2006**, *9* (10), 46. (vii) in het Panhuis, M. *J. Mater. Chem.* **2006**, *16*, 3598. (viii) Snow, E. S.; Perkins, F. K.; Robinson, J. A. *Chem. Soc. Rev.* **2006**, *35*, 790. (ix) Moniruzzaman, M.; Winey, K. I. *Macromolecules* **2006**, *39*, 5194. (x) Lau, K.-T.; Gu, C.; Hui, D. *Composites, Part B* **2006**, *37B*, 425.

(2) For DWNT, see: (i) Bandow, S.; Takizawa, M.; Hirahara, K.; Yudasaka, M.; Iijima, S. *Chem. Phys. Lett.* **2001**, *337*, 48. (ii) Hutchison, J. L.; Kiselev, N. A.; Krinichnaya, E. P.; Krestinin, A. V.; Loutfy, R. O.; Morawsky, A. P.; Muradyan, V. E.; Obraztsova, E. D.; Sloan, J.; Terekhov, S. V.; Zakharov, D. N. *Carbon* **2001**, *39*, 761. (iii) Bacsa, R. R.; Peigney, A.; Laurent, C. H.; Puech, P.; Bacsa, W. S. *Phys. Rev. B* **2002**, *65*, 161404. (iv) Nagy, C. L.; Diudea, M. V.; Balaban, T. S. *Nanostructures* **2005**, *25*. (v) Sugai, T. *New Diamond Front. Carbon Technol.* **2006**, *16*, 151. (vi) Yamada, T.; Namai, T.; Hata, K.; Futaba, D. N.; Mizuno, K.; Fan, J.; Yudasaka, M.; Yumura, M.; Iijima, S. *Nat. Nanotechnol.* **2006**, *1*, 131.

(3) For FWNT, see: (i) Gohier, A.; Minea, T. M.; Djouadi, M. A.; Granier, A. *J. Appl. Phys.* **2007**, *101*, 054317. (ii) Gohier, A.; Minea, T. M.; Djouadi, M. A.; Jimenez, J.; Granier, A. *Phys. E* **2007**, *37*, 34. (iii) Qian, C.; Qi, H.; Liu, J. *J. Phys. Chem. C* **2007**, *111*, 131. (iv) Qi, H.; Qian, C.; Liu, J. *Chem. Mater.* **2006**, *18*, 5691. (v) Qian, C.; Qi, H.; Gao, B.; Cheng, Y.; Qiu, Q.; Qin, L.-C.; Zhou, O.; Liu, J. *J. Nanosci. Nanotechnol.* **2006**, *6*, 1346. (vi) Ramesh, P.; Sato, K.; Ozeki, Y.; Yoshikawa, M.; Kishi, N.; Sugai, T.; Shinohara, H. *NANO* **2006**, *207*. (vii) Qian, C.; Qi, H.; Gao, B.; Zhou, O.; Liu, J. *PMSE Prepr.* **2005**, *92*, 516.

10.1021/cm702857z CCC: $40.75
Published on Web 01/17/2008

because of the technological opportunities that their thermal, electrical, mechanical, and optical properties could offer. These nanomaterials are being actively investigated with respect to their structural reinforcement, energy/electron transport or storage capabilities, and interactions with electromagnetic waves as well as the efficient ways to transfer their outstanding properties to the polymeric matrices. A common goal is to make the resulting polymer nanocomposites for advanced applications that are affordable, lightweight, and multifunctional. While most of the initial studies have focused on SWNTs, vapor-grown carbon nanofibers (VGCNFs), which are structurally hollow and multiwalled but several orders of magnitude larger in diameter and length than MWNT and SWNT, are more practical in terms of their relatively low cost and availability in greater quantities as a result of their more advanced stage in commercial production.[4–6] These carbon nanofibers (CNFs) are typically produced by a vapor-phase catalytic process in which a carbon-containing feedstock (e.g., CH_4, C_2H_2, C_2H_4, etc.) is pyrolyzed in the presence of a small metal catalyst (e.g., ferrocene, $Fe(CO)_5$, etc.) and has an outer diameter of 60–200 nm, a hollow core of 30–90 nm, and a length on the order of 50–100 μm.[7,8] It follows that having aspect ratios (length/diameter) of greater than 800 should make them useful as a nanolevel reinforcement for polymeric matrixes. Furthermore, because their inherent electrical and thermal transport properties are also excellent, there are many innovative possibilities for tailoring their polymer matrix composites into cost-effective, multifunctional materials. We have also rationalized that the similarity in the chemical and structural features between CNFs and MWNTs, viz., the structural defects, should allow an easy translation of synthetic tools and scale-up processes developed for VGCNF to more expensive DWNT, FWNT, or MWNT.

Following the success in improving the effectiveness of the Friedel–Crafts (F−C) acylation reaction in an optimized mixture of poly(phosphoric acid) and phosphorus pentoxide (PPA/P_2O_5) in poly(ether ketone) (PEK) synthesis and exploring the generality of this polymer-forming process,[9] we then extended its application to surface modifications of CNF and MWNT with carbonyl-based aromatic moieties as well as linear PEKs.[10] Apart from being an efficient F–C catalyst, the PPA/P_2O_5 medium is moderately acidic but effective enough to promote homogeneous dispersion of CNF and MWNT at relatively low temperature, avoiding the premature onset of the F–C reaction, and its relatively high viscosity impedes reaggregation of CNF and MWNT. As a result, a uniform grafting of linear PEKs onto CNF and MWNT has been achieved via this in situ polymerization method. However, these materials were found to be more soluble in strong acids than in common organic solvents. This finding has prodded us to explore the use of an "aromatic hyperbranched polymer" approach to improving the solubilization of CNFs and CNTs. This is because high solubility (or nanodispersibility) in organic and aqueous solvents is an important prerequisite to the processing and fabrication of these materials on large surface areas. Furthermore, the nonentangling nature of hyperbranched structures should also aid in controlling the solution or melt viscosity during the processing of the resulting materials.

Various in situ polymerization methods in grafting hyperbranched polymers to or from the surfaces of CNFs[11] and CNTs have been reported in the literature: (a) atom-transfer radical polymerization;[12] (b) ring-opening polymerization;[13] (c) self-condensing vinyl polymerization;[14] (d) polycondensation.[15] In a recent example, SWNT was grafted with poly(aminoamine)-type dendrimers using a divergent methodology.[16] In all cases, (a) the CNF/CNT surfaces were prefunctionalized with appropriate functional groups (e.g., initiators) for the subsequent polymerization processes and (b) either aliphatic or partially aliphatic hyperbranched polymers resulted. In our case, no such prefunctionalization was required, and the resulting HPB-PEK is wholly aromatic, which will allow higher use temperatures.

We have reported the initial results of this effort,[17] and herein we present a more comprehensive account of our investigation.

Experimental Section

Materials. All reagents and solvents were purchased from Aldrich Chemical Co. Inc. and used as received, unless otherwise specified. VGCNFs (PR-19-HT) were procured from Applied Science Inc., Cedarville, OH, via an Air Force contract.

Instrumentation. Proton and carbon nuclear magnetic resonance (^{1}H NMR and ^{13}C NMR) spectra for intermediates and the A_2B monomer were measured at 270 and 50 MHz on a JEOL 270 spectrometer. ^{1}H NMR spectra of polymer composites were measured at 400 MHz on a Bruker AVANCE 400 spectrometer. Infrared (IR) spectra were recorded on a Nicolet Nexus 470 Fourier transform spectrophotometer. Elemental analysis and mass spectral analysis (ThermoQuest-Finnigan TSQ 7000 mass spectrometer using electron impact ionization mode) were performed by System Support Branch, Materials Directorate, Air Force Research Laboratory, Dayton, OH. The melting points (mp's) of all compounds were

(4) Applied Sciences, Inc., Cederville, OH. http://www.apsci.com.
(5) Rodriguez, N. M. *J. Mater. Res.* **1993**, *8*, 233.
(6) Maruyama, B.; Alam, K. *SAMPE J.* **2002**, *38*, 59.
(7) Carneiro, O. S.; Covas, J. A.; Bernardo, C. A.; Caldeira, G.; Hattum, F. W. J. V.; Ting, J. M.; Alig, R. L.; Lake, M. L. *Compos. Sci. Technol.* **1998**, *58*, 401.
(8) Singh, C.; Quested, T.; Boothroyd, C. B.; Thomas, P.; Kinloch, I. A.; Abou-Kandil, A. I.; Windle, A. H. *J. Phys. Chem. B* **2002**, *106*, 10915.
(9) (a) Baek, J.-B.; Tan, L.-S. *Polymer* **2003**, *44*, 4135. (b) Baek, J.-B.; Park, S.-Y.; Price, G. E.; Lyons, C. B.; Tan, L.-S. *Polymer* **2005**, *46* (5), 1543.
(10) (a) Baek, J.-B.; Lyons, C. B.; Tan, L.-S. *J. Mater. Chem.* **2004**, *14*, 2052. (b) Baek, J.-B.; Lyons, C. B.; Tan, L.-S. *Macromolecules* **2004**, *37*, 8278. (c) Lee, H.-J.; Oh, S.-J.; Choi, J.-Y.; Kim, J. W.; Han, J.; Tan, L.-S.; Baek, J.-B. *Chem. Mater.* **2005**, *17*, 5057. (d) Oh, S.-J.; Lee, H.-J.; Keum, D.-K.; Lee, S.-W.; Wang, D. H.; Park, S.-Y.; Tan, L.-S.; Baek, J.-B. *Polymer* **2006**, *47*, 1132.
(11) Rhodes, S. M.; Higgins, B.; Xu, Y.; Brittain, W. J. *Polymer* **2007**, *48*, 1500.
(12) (i) Gao, C.; Muthukrishnan, S.; Li, W.; Yuan, J.; Xu, Y.; Mueller, A. H. E. *Macromolecules* **2007**, *40*, 1803. (ii) Cao, L.; Yang, W.; Yang, J.; Wang, C.; Fu, S. *Chem. Lett.* **2004**, *33*, 490.
(13) Xu, Y.; Gao, C.; Kong, H.; Yan, D.; Jin, Y. Z.; Watts, P. C. P. *Macromolecules* **2004**, *37*, 8846.
(14) Hong, C.-Y.; You, Y.-Z.; Wu, D.; Liu, Y.; Pan, C.-Y. *Macromolecules* **2005**, *38* (7), 2606.
(15) Yang, Y.; Xie, X.; Wu, J.; Yang, Z.; Wang, X.; Mai, Y.-W. *Macromol. Rapid Commun.* **2006**, *27*, 1695.
(16) Campidelli, S.; Sooambar, C.; Diz, E. L.; Ehli, C.; Guldi, D. M.; Prato, M. *J. Am. Chem. Soc.* **2006**, *128*, 12544.
(17) Wang, D. H.; Baek, J.-B.; Tan, L.-S. *Polym. Sci. Eng. B* **2006**, *132*, 103.

determined on a Mel-Temp melting point apparatus and are uncorrected. Intrinsic viscosities were determined with a Cannon-Ubbelohde No. 75 viscometer. Flow times were recorded for an *N*-methyl-2-pyrrolidinone (NMP) solution with 1 wt % lithium bromide and polymer concentrations of approximately 0.5–0.10 g/dL at 30.0 ± 0.1 °C. Differential scanning calorimetry (DSC) analyses were performed in nitrogen with a heating rate of 10 °C/min using a Perkin-Elmer model 2000 thermal analyzer equipped with a DSC cell. Thermogravimetric analysis (TGA) was conducted in nitrogen (N_2) and air atmospheres at a heating rate of 10 °C/min using a TA Hi-Res TGA 2950 themogravimetric analyzer. The scanning electron microscope used in this work was a Hitachi S-5200 instrument. Transmission electron microscopy (TEM) experiments were conducted using a JEOL 2000FX microscope with an accelerating voltage of 120 kV. Sonication was conducted at 20 kHz with 600 W of power using an Ace Glass GEX 600-5 ultrasonic processor.

The A_2B monomer (**2**), 5-phenoxyisophthalic acid,[18] was synthesized in a two-step sequence, following slightly modified literature procedures.

1,3-Dimethyl-5-phenoxybenzene.[18,19] Into a 250 mL three-necked, round-bottom flask equipped with a magnetic stirbar, a nitrogen inlet, and a Dean–Stark trap were charged phenol (61.0 g, 0.648 mol), toluene (60 mL), and KOH (30.3g, 0.540 mol), and the resulting mixture was heated at 145 °C for 3 h with water collected in the Dean–Stark trap. Then, excess phenol and water were removed under reduced pressure at 160 °C for 3 h. Copper (1.0 g), 5-bromo-*m*-xylene (20.0 g, 0.108 mol), and phenol (30 mL) were added to the dry salt. The mixture was agitated under dry nitrogen at 220 °C for 3 h. The reaction mixture was poured slowly into water (2000 mL), and a 5 wt % NaOH solution was added to dissolve the excess phenol. The mixture was extracted with ethyl acetate (3 × 700 mL). The combined extract was dried and evaporated to dryness. The product was further purified by column chromatography (eluent CH_2Cl_2/hexane, 1:7) to afford 19.9 g (93%) of a colorless liquid. Anal. Calcd for $C_{14}H_{14}O$: C, 84.81; H, 7.12. Found: C, 84.59; H, 7.39. FT-IR (KBr, cm^{-1}): 3039, 2918, 1614, 1585, 1490, 1299, 1220, 1163, 1136, 1027, 950, 850, 756. MS (*m*/*e*): 198 (M^+, 100% relative abundance). ^{1}H NMR ($CDCl_3$, δ in ppm): 2.25 (s, 6H), 6.62 (s, 2H), 6.71 (s, 1H), 6.96 (d, 2H), 7.04 (t, 1H), 7.28 (dd, 2H). ^{13}C NMR ($CDCl_3$, δ in ppm): 21.25, 116.60, 118.79, 122.91, 124.95, 129.62, 139.49, 157.12, 157.41.

5-Phenoxyisophthalic Acid[18,20] **(2).** Into a 1-L three-necked, round-bottom flask equipped with a magnetic stirbar, a nitrogen inlet, and a condenser were placed 1,3-dimethyl-5-phenoxybenzene (18.0 g, 90.8 mmol), water (140 mL), and pyridine (350 mL), and the resulting mixture was heated to 100 °C. Potassium permanganate (160 g, 1.02 mol) was added in small portions over a 6-h period. Then the mixture was agitated at 120 °C for 36 h. The by-product, manganese dioxide, was removed by filtration and washed several times with hot water. The combined filtrate was acidified with a dilute HCl solution. The product was collected by filtration and recrystallized from acetic acid to afford 18.0 g (77%) of white crystals. Mp: 301–303 °C (lit. mp not reported). Anal. Calcd for $C_{14}H_{10}O_5$: C, 65.12; H, 3.90. Found: C, 64.93; H, 4.09. FT-IR (KBr, cm^{-1}): 3421, 2826 (br, COOH), 2568, 1690 (*C*═O), 1586, 1491, 1320, 1281, 1202, 974, 757. MS (*m*/*e*): 258 (M^+, 100% relative abundance). ^{1}H NMR ($CDCl_3$ + DMSO-d_6, δ in ppm): 7.05 (d, 2H), 7.17 (t, 1H), 7.39 (dd, 2H), 7.80 (d, 2H), 8.40 (t, 1H), 8.82 (br s, 2H). ^{13}C NMR ($CDCl_3$ + DMSO-d_6, δ in ppm): 119.22, 123.14, 124.09, 125.38, 129.99, 133.01, 156.05, 157.46, 166.85.

Representative Procedure for in Situ Polymerization [20 wt % (HBP-PEK)-*g*-VGCNF (3f)]. Into a 250-mL resin flask equipped with a high-torque mechanical stirrer and nitrogen inlet and outlet were charged 5-phenoxyisophthalic acid (3.20 g, 12.4 mmol), VGCNF (0.80 g), and PPA (83% P_2O_5 assay, 80 g), and the resulting mixture was stirred with dried nitrogen purging at 130 °C for 4 h. Phosphorus pentoxide (P_2O_5, 20 g) was added in one portion. The initially dark mixture became lighter and more viscous as the hyperbranching polymerization process progressed. After 12 h at 130 °C, the reaction mixture was so viscous that it would stick to the stirring rod during rapid stirring. The temperature was maintained at 130 °C for 48 h. At the end of the reaction, water was added into the flask. The resulting black polymer clusters were put into a Waring blender, and the polymer bundles were chopped, collected by suction filtration, and Soxhlet-extracted with water for 3 days and methanol (to remove, if any, the residual A_2B monomer) for 3 days more. It was then dried over P_2O_5 under reduced pressure at 120 °C for 72 h to afford 3.60 g (95.3% based on a theoretical yield of 3.78 g) of a black powder.

The calculation of the theoretical yield is as follows:

$$\text{theoretical yield (g)} = 4.0 \text{ g of} \times \frac{\text{FW of } C_{14+n}H_8O_4}{\text{FW of } C_{14+n}H_{10}O_5}$$

The amount of 4.0 g is the total weight of 5-phenoxyisophthalic acid and VGCNF used. $C_{14+n}H_{10}O_5$ is the formula of the 5-phenoxyisophthalic acid and VGCNF mixture before polymerization. $C_{14+n}H_8O_4$ and $C_{14}H_8O_4$ are the empirical formulas of the (HBP-PEK)-*g*-VGCNF and PEK repeat units, respectively.

Anal. Calcd for $C_{19.38}H_8O_4$: C, 76.37; H, 2.63; O, 21.00. Found: C, 76.04; H, 2.79; O, 19.55. FT-IR (KBr, cm^{-1}): 3425, 3071, 1721 (COOH), 1659 (*C*═O), 1584, 1501, 1413, 1237, 1163, 760.

Samples, 3b, 3c, 3d, 3e, 3g, and 3 h were prepared and worked up following the same procedure as that described above with the amounts of starting materials used and the product yields listed below. The empirical formulas and results for elemental analysis of each sample can be found in Table 2. A similar set of FT-IR bands in KBr cells as those for **3f** were also found for these samples.

1 wt % (HBP-PEK)-*g*-VGCNF (3b). 5-Phenoxyisophthalic acid (3.96 g, 15.3 mmol), VGCNF (0.04 g), PPA (80 g), and P_2O_5 (20 g) were used. Yield: 3.49 g (93.7% based on 3.72 g of the theoretical product).

2 wt % (HBP-PEK)-*g*-VGCNF (3c). 5-Phenoxyisophthalic acid (3.92 g, 15.2 mmol), VGCNF (0.08 g), PPA (80 g), and P_2O_5 (20 g) were used. Yield: 3.48 g (93.4% based on 3.73 g of the theoretical product).

5 wt % (HBP-PEK)-*g*-VGCNF (3d). 5-Phenoxyisophthalic acid (3.80 g, 14.7 mmol), VGCNF (0.20 g), PPA (80 g), and P_2O_5 (20 g) were used. Yield: 3.56 g (95.6% based on 3.72 g of the theoretical product).

10 wt % (HBP-PEK)-*g*-VGCNF (3e). 5-Phenoxyisophthalic acid (3.60 g, 13.9 mmol), VGCNF (0.40 g), PPA (80 g), and P_2O_5 (20 g) were used. Yield: 3.55 g (94.7% based on 3.75 g of the theoretical product).

30 wt % (HBP-PEK)-*g*-VGCNF (3g). 5-Phenoxyisophthalic acid (2.80 g, 10.8 mmol), VGCNF (1.20 g), PPA (80 g), and P_2O_5 (20 g) were used. Yield: 3.59 g (94.5% based on 3.80 g of the theoretical product).

40 wt % (HBP-PEK)-*g*-VGCNF (3h). 5-Phenoxyisophthalic acid (2.40 g, 9.29 mmol), VGCNF (1.60 g), PPA (80 g), and P_2O_5 (20 g) were used. Yield: 3.54 g (92.4% based on 3.83 g of the theoretical product).

(18) Shu, C.-F.; Leu, C.-M. *Macromolecules* **1999**, *32*, 100.
(19) Smith, K.; Jones, D. *J. Chem. Soc., Perkin Trans. 1* **1992**, (4), 407.
(20) Melendez, A.; De la Campa, J. G.; De Abajo, J. *Polymer* **1988**, *29* (6), 1142.

Table 1. VGCNF/A_2B Monomer Feed Ratio, Calculated and TGA-Determined VGCNF/HBP-PEK Composition, Intrinsic Viscosity, and Elemental Analysis Data

	feed		calcd		found[a]			elem anal.		
sample	VGCNF (wt %)	HBP-PEK (wt %)	VGCNF (wt %)	HBP-PEK (wt %)	VGCNF (wt %)	$[\eta]^b$ (dL/g)		C (%)	H (%)	O (%)
1	100	0	100	0	99.8		calcd[c]	100	0	0
							found	99.02	1.01	<0.1
3a	0	100	0	100	0.7	0.34	calcd[c]	70.00	3.36	26.63
							found	69.54	3.47	26.23
3b	1	99	1.1	98.9	1.4	0.42	calcd[c]	70.34	3.32	26.34
							found	69.60	3.29	27.01
3c	2	98	2.2	97.8	2.6	0.47	calcd[c]	70.67	3.29	26.04
							found	70.47	3.32	26.23
3d	5	95	5.4	94.6	5.2	0.57	calcd[c]	71.62	3.15	25.22
							found	71.48	3.10	23.93
3e	10	90	10.7	89.3	11.0	0.82	calcd[c]	73.22	2.98	23.81
							found	72.94	3.12	21.74
3f	20	80	21.2	78.8	22.1	1.46	calcd[c]	76.37	2.63	21.00
							found	76.08	2.79	19.55
3g	30	70	31.5	68.5	31.3	2.45	calcd[c]	77.88	2.32	18.39
							found	77.53	2.23	18.81
3h	40	60	41.8	58.2	42.1	4.89	calcd[c]	82.00	2.01	15.99
							found	81.82	2.10	16.47
4	7.1	92.9	7.9	92.1	8.2	0.64	calcd[c]	71.92	2.94	12.84
							found	72.44	3.18	12.53
5	6.4	93.6	6.9	93.1	6.9	0.56	calcd[c]	78.03	7.32	14.65
							found	78.54	7.61	13.93
6	11.1	88.9	11.8	88.2	10.3	0.67	calcd[c]	77.07	3.75	13.34
							found	76.81	3.88	12.97
7			10.7	89.3	10.2		calcd[c]	73.22	2.98	23.81
							found	72.45	3.22	25.75

[a] Residual weight percentage at 650 °C from TGA thermograms in air. [b] Intrinsic viscosity measured in NMP at 30.0 ± 0.1 °C. [c] A_2B repeat unit $C_{14}H_8O_4$ and calculated repeat units as follows: **3a** (100:0), $C_{14}H_8O_4$; **3b** (1:99), $C_{14.23}H_8O_4$; **3c** (2:98), $C_{14.45}H_8O_4$; **3d** (5:95), $C_{15.13}H_8O_4$; **3e** (10:90), $C_{16.39}H_8O_4$; **3f** (20:80), $C_{19.38}H_8O_4$; **4g** (30:70), $C_{22.59}H_8O_4$; **3f** (40:60), $C_{27.33}H_8O_4$; **5**, $C_{22.39}H_{11}NO_3S$; **6**, $C_{28.39}H_{32}O_4$; **7**, $C_{15.39}H_9NO_2$. The formula of (HBP-PEK)-*g*-VGCNF is $C_{14+n}H_8O_4$. $C_{14}H_8O_4$ is the formula of the PEK repeat unit. The subscript *n* is the number of VGCNF carbons per PEK repeat unit and is calculated as follows:

$$n = \left(\frac{\text{weight percentage of VGCNF}}{12.011}\right) \Big/ \left(\frac{\text{weight percentage of HBP-PEK}}{240.22}\right)$$

where 12.011 is the VGCNF formula (C) molecular weight and 240.22 is the molecular weight of the HBP-PEK repeat unit.

Extraction of Free HBP-PEK from 20 wt % (HBP-PEK)-*g*-VGCNF. Free HBP-PEK is only slightly soluble in hot methanol, but it is very soluble in tetrahydrofuran (THF). Therefore, **3f** (powder sample, 1.00 g) was submerged in THF in a closed vial at room temperature for 48 h. During this period, the suspension was sonicated followed by centrifuging, and then the top part of the clear solution in each vial was carefully withdrawn by a disposable pipette. The vial was then replenished with fresh THF. The THF extract was spotted on a thin-layer chromatography (TLC) plate and checked for fluorescence due to HBP-PEK with a hand-held UV lamp. The above extraction routine was repeated three times until TLC showed no sign (fluorescent spot) of free HBP-PEK in the THF extract. After removal of THF from the sample, the residue was dried in vacuum to afford 0.98 g of a black powder. This test indicates that most of HBP-PEK was grafted onto VGCNF. Together with the result from Soxhlet extraction, it is estimated that 5–7 wt % of free HBP-PEK is present in the as-synthesized (HBP-PEK)-*g*-VGCNF nanocomposites as the upper limit.

PPA-Treated VGCNF. PPA-treated VGCNF was prepared from VGCNF (0.50 g), PPA (83% P_2O_5 assay, 20 g), and P_2O_5 (5.0 g) following the same procedure as that used for the synthesis of **3e** to afford 0.47 g (94% yield based on the initial amount) of a black solid. Found: C, 98.66; H, 0.93; N, <0.20; O, <0.10.

Benzothiazole-Terminated (HBP-PEK)-*g*-VGCNF (4). Into a 250-mL resin flask equipped with a high-torque mechanical stirrer and nitrogen inlet and outlet were charged **3e** (4.0 g, 10.1 mmol), 2-aminothiophenol (3.5 g, 28.0 mmol), P_2O_5 (20 g), and PPA (83% P_2O_5 assay, 80 g), and the resulting mixture was stirred with dry nitrogen purging at 150 °C for 24 h. At the end of the reaction, water was added into the flask. The resulting black polymeric clusters were put into a Waring blender, and the polymer bundles were chopped, collected by suction filtration, and Soxhlet-extracted with water for 3 days and methanol for 3 days. It was then dried over P_2O_5 under reduced pressure at 120 °C for 72 h to give the product in quantitative yield. Anal. Calcd for $C_{22.39}H_{11}NO_3S$: C, 71.92; H, 2.94; N, 3.74; O, 12.84. Found: C, 72.44; H, 3.55; N, 3.98; O, 12.53. FT-IR (KBr, cm^{-1}): 3452, 3057, 1660 (*C*═O), 1604, 1581, 1500, 1311, 1222, 1166, 757.

Dodecyl-Terminated (HBP-PEK)-*g*-VGCNF (5). Into a 100-mL three-necked flask equipped with a mechanical stirrer and nitrogen inlet and outlet were charged **3e** (2.0 g, 5.04 mmol), 1-dodecanol (4.0 g, 21.4 mmol), *N*,*N*′-dicyclohexylcarbodiimide (DCC; 2.10 g, 10.2 mmol), 4-(*N*,*N*-dimethylamino)pyridine (DMAP; 0.2 g), and *N*,*N*-dimethylformamide (DMF; 200 mL), and the resulting mixture was stirred with dried nitrogen purging at room temperature for 3 days. At the end of the reaction, the mixture was poured into water. The resulting black polymeric material was collected by suction filtration and Soxhlet-extracted with methanol for more 3 days. It was then dried over P_2O_5 under reduced pressure at 120 °C for 72 h to give the product in a quantitative yield. Anal. Calcd for $C_{28.39}H_{32}O_4$: C, 78.67; H, 7.32; O, 13.93. Found: C, 79.66; H, 7.76; O, 14.65. FT-IR (KBr, cm^{-1}): 2925, 2854, 1723 (ester), 1660 (*C*═O), 1582, 1232, 1163, 1002, 991.

Amine-Terminated (HBP-PEK)-*g*-VGCNF (6). Into a 100-mL resin flask equipped with a high-torque mechanical stirrer and nitrogen inlet and outlet were charged compound **3e** (1.0 g, 2.52 mmol) and methanesulfonic acid (MSA; 6.7 g), and the resulting mixture was stirred with dry nitrogen purging at room temperature.

Scheme 1. In Situ Polymerization of 3,5-Diphenoxybenzoic Acid with VGCNF and Its Post Polymer Functionalization[a]

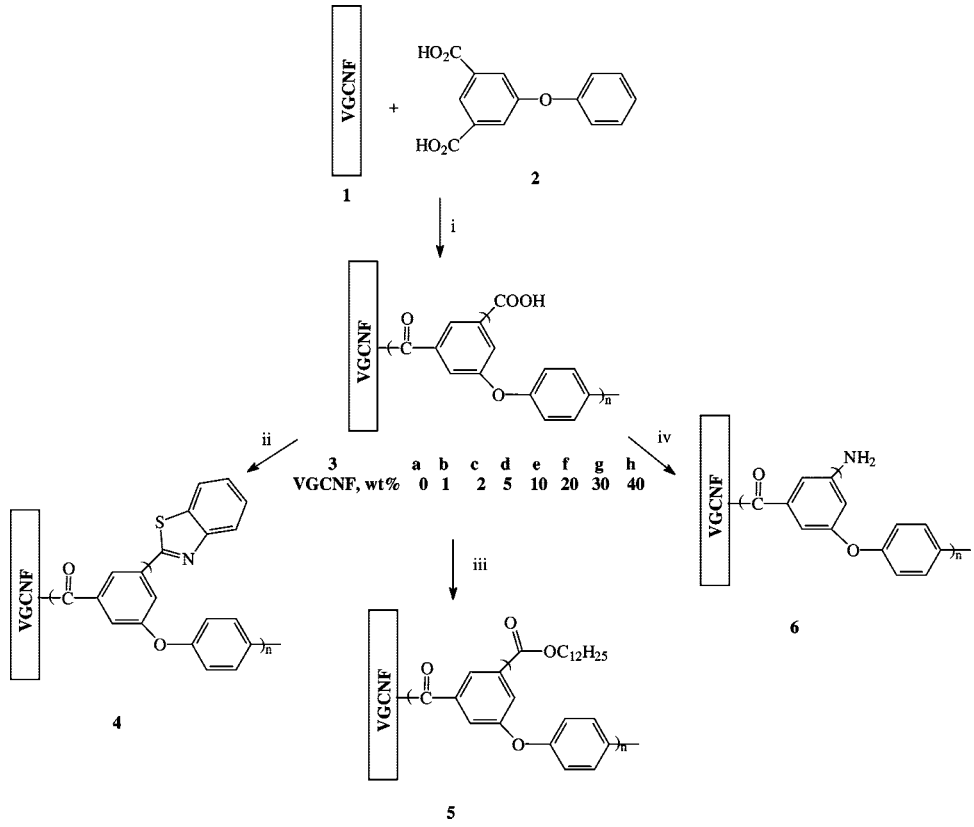

[a] (i) PPA/P_2O_5, 130 °C. (ii) PPA/P_2O_5, 2-aminothiophenol, 150 °C. (iii) 1-Dodecanol, DCC, DMAP, DMF. (iv) Sodium azide, MSA. Note that the structures of (HBP-PEK)-*g*-VGCNF and it derivatives are idealized.

Sodium azide (0.19 g, 2.52 mmol) was added in several portions over 4 h. The mixture was stirred at room temperature for 3 days and then was poured into methanol. The resulting black polymeric material was collected by suction filtration and Soxhlet-extracted with water for 3 days and methanol for 3 days more. It was then dried over P_2O_5 under reduced pressure at 120 °C for 72 h to give the product in a quantitative yield. Anal. Calcd for $C_{15.39}H_9NO_2$: C, 77.07; H, 3.75; O, 13.34. Found: C, 77.82; H, 3.86; O, 12.97. FT-IR (KBr, cm^{-1}): 3441, 3384 (NH_2), 3027, 1647 (*C*=O), 1581, 1384, 1239, 1165.

HBP-PEK/VGCNF Blends (10 wt % VGCNF; 7). Into a 100-mL three-necked, round-bottom flask equipped with a magnetic stirbar and nitrogen inlet were charged **3a** (1.786 g), VGCNF (0.214 g), and MSA (0 mL), and the resulting mixture was heated at 50 °C for 24 h. The mixture was allowed to cool to room temperature and poured into water. The resulting black powder was collected by suction filtration and Soxhlet-extracted with water for 3 days and methanol for 3 days. It was then dried over P_2O_5 under reduced pressure at 120 °C for 72 h to give the product in a quantitative yield. Anal. Calcd for $C_{16.39}H_8O_4$: C, 73.22; H, 2.98; O, 23.81. Found: C, 72.45; H, 3.22; O, 25.75.

Results and Discussion

In Situ Polycondensation and Chain-End Modification. The as-received VGCNF contains a significant amount of hydrogen, about 1 wt % as judged by elemental analysis results and IR spectral data. This hydrogen content is presumably attributable to the sp^3 and sp^2 C−H and may be related to the use of methane as the major component in the feedstock for VGCNF production. Previously, we demonstrated that VGCNF could be functionalized via F–C acylation with a model compound, 2,4,6-trimethylphenoxybenzoic acid, in PPA/P_2O_5.[10a] The degree of functionalization, reported as the number of defect C−H sites that were arylcarbonylated per 100 carbon atoms, was determined to be ~3 atom % by the combination of TGA and elemental analysis. In this work, the in situ polymerization (Scheme 1) of the A_2B monomer, 5-phenoxyisophthalic acid (**2**), in the presence of dispersed VGCNF was carried out with varied VGCNF contents (0, 1, 2, 5, 10, 20, 30, and 40 wt %) to yield the carboxylic acid terminated **3a**−**h**. In a typical

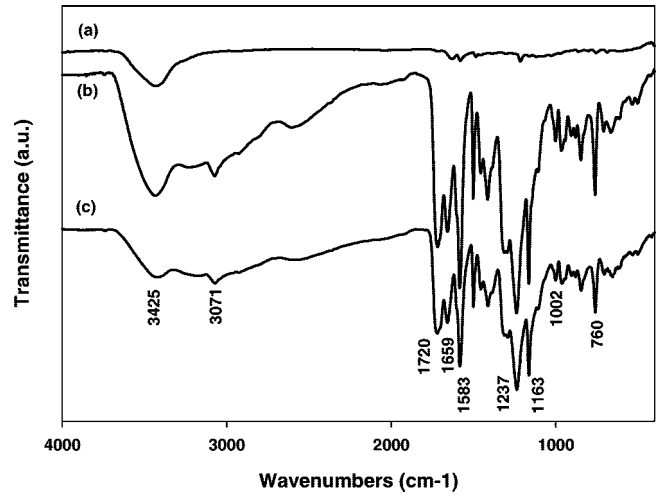

Figure 1. Composite FT-IR spectra of (a) VGCNF **5**, (b) HBP-PEK **6a**, (c) 10 wt % (HBP-PEK)-*g*-VGCNF **6e**.

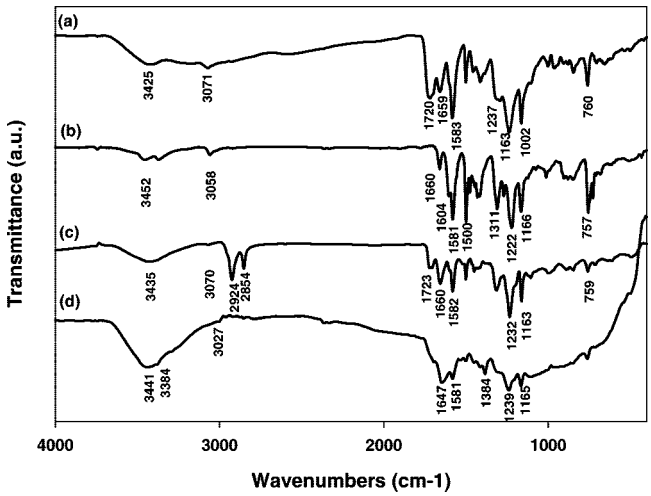

Figure 2. Composite FT-IR spectra of **3e**: (a) carboxylic acid terminated; (b) benzothiazole-terminated; (c) dodecyl-terminated; (d) amine-terminated.

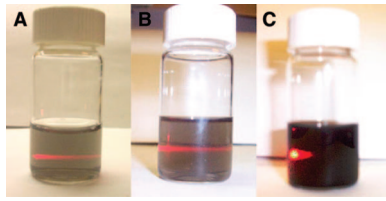

Figure 3. Using a red laser pointer (aiming from the left side of each sample bottle) to qualitatively assess the optical transparency of various solutions of 10 wt % (HPB-PEK)-g-VGCNF (**3e**) dissolved in 10 wt % aqueous NH_4OH: (A, 1 wt % **3e**; B, 2 wt % **3e**; C, 5 wt % **3e**).

Table 2. Solubility Testing Results of (HBP-PEK)-*g*-VGCNF[a]

sample	MSA	NMP	DMAc	ethanol/ ethanol	TEA	NH_4OH	DCB	$CHCl_3$
3a−3h	+	+	+	±	+	+	−	−
4	+	+	+	±	−	−	+	−
5	−	−	−	−	−	−	+	+
6	+	+	+	±	−	−	−	−

[a] MSA: methanesulfonic acid. NMP: 1-methyl-2-pyrrolidinone. DMAc: dimethylacetamide. TEA: triethylamine. DCB: dichlorobenzene. + indicates solubility of at least 1.0 g/dL at room temperature. ± indicates 0.1 g/dL < solubility < 1.0 g/dL at room temperature. − indicates solubility < 0.1 g/dL at room temperature.

preparation, VGCNF and the A_2B monomer were first mechanically stirred and dispersed into PPA at 130 °C for 4 h. P_2O_5 was then added to enhance the acidity and catalytic potency of PPA and to accelerate the polymerization and grafting of the A_2B monomer to VGCNF surfaces, which most likely took place concurrently. The homogeneous solutions became viscous overnight. The polymerization mixture (dope) remained fluid (but would climb up the stirring rod upon rapid stirring) at the end of each synthesis run. We previously observed that when a linear PEK analogue was synthesized in the presence of VGCNF, the maximal amount of VGCNF incorporated into nanocomposites was 30 wt %. Higher concentrations led to a bulk viscosity that was too high for efficient mechanical stirring during the final stage of polymerization.[10b] However, in this work, even at 40 wt %, (HBP-PEK)-*g*-VGCNF has been prepared without any stirring difficulty caused by the high bulk viscosity. We attribute this improvement to the non-

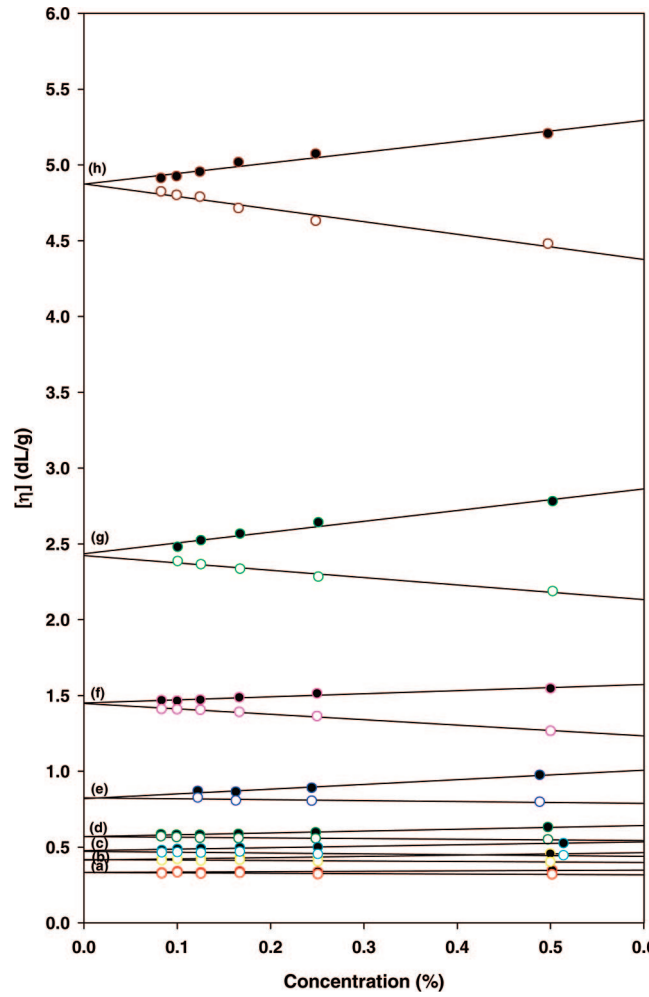

Figure 4. Inherent viscosity (solid dots) and reduced viscosity (unfilled circles): (a) HBP-PEK, **6a** (red circles); (b) 1 wt % (HBP-PEK)-*g*-VGCNF, **6b** (yellow circles); (c) 2 wt % (HBP-PEK)-*g*-VGCNF, **6c** (cyan circles); (d) 5 wt % (HBP-PEK)-*g*-VGCNF, **6d** (dark-green circles); (e) 10 wt % (HBP-PEK)-*g*-VGCNF, **6e** (blue circles); (f) 20 wt % (HBP-PEK)-*g*-VGCNF, **6f** (pink circles); (g) 30 wt % (HBP-PEK)-*g*-VGCNF, **6g** (green circles); (h) 40 wt % (HBP-PEK)-g-VGCNF, **6f** (dark-red circles).

entangling nature of HPB-PEK. For comparison purposes, a 10 wt % physical blend (**7**) of HBP-PEK (**3a**) and VGCNF (**1**) was also prepared by mixing in MSA at 50 °C.

The presence of a myriad of carboxylic groups at the periphery of the HBP-PEK component provided an opportunity to evaluate the feasibility in post polymer functionalization of the materials and controllable changes in the physical properties resulting from such a chain-end modification. In these studies, the carboxylic acid terminated (HBP-PEK)-*g*-PEK (**3e**, 10 wt % of VGCNF) was further functionalized with a benzothiazole (**4**), a dodecyl ester (**5**), and an aromatic amine (**6**), respectively, under appropriate reaction conditions (Scheme 1). Thus, **3e** was condensed with *o*-aminothiophenol in PPA/P_2O_5 at 150 °C to afford the benzothiazole-terminated **4**. **3e** was esterified with 1-dodecanol in the presence of DCC as a dehydrating agent and DMAP as a catalyst to give the dodecyl ester terminated **5**. The amine-terminated analogue (**6**) was obtained via a Schmidt reaction by treating **3e** with sodium azide in MSA at room temperature.[21] After isolation, (HPB-PEK)-*g*-VGCNF dissolved more easily in MSA at room temperature than it did in PPA, so we used MSA as the solvent for this

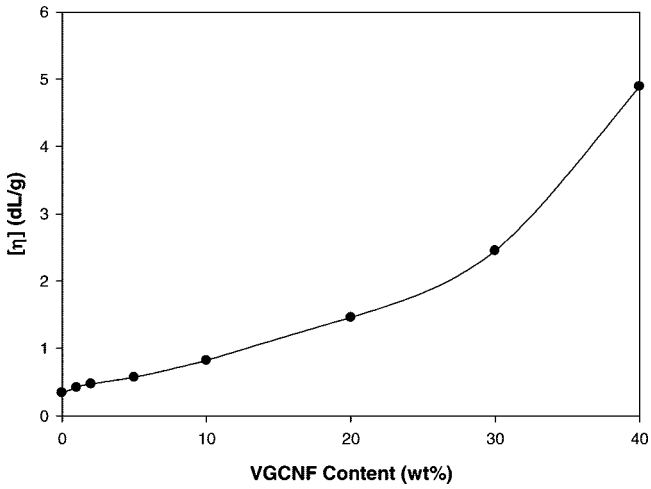

Figure 5. Plot of the intrinsic viscosity of (HBP-PEK)-*g*-VGCNFsvs VGCNF content.

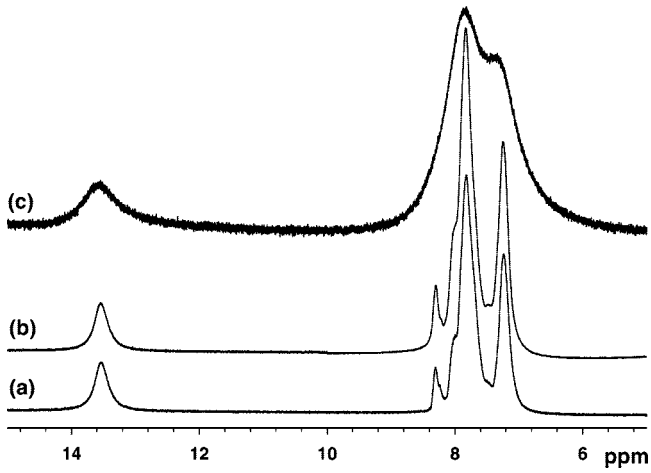

Figure 6. ^{1}H NMR spectra (DMSO-d_6) of (a) HBP-PEK, (b) 10 wt % (HBP-PEK)/VGCNF blend, and (c) 10 wt % (HBP-PEK)-*g*-VGCNF.

chemical modification. It is also possible that the Schmidt reaction on CO_2H-terminated (HPB-PEK)-*g*-VGCNF can be performed in a one-pot fashion immediately after the polycondensation process. Together these results illustrate good functionalization flexibility in our synthesis strategy because both one-pot and two-stage chain-end functionalization modes of (HBP-PEK)-*g*-VGCNF are possible. It is noteworthy that in all of the in situ polymerization and chain-end modification experiments, we did not observe any gel formation arising from a cross-linking reaction among the polymer-grafted VGCNF. In theory, one would expect the occurrence of a cross-linking reaction during the in situ polymerization because of the presence of multiple reactive sites on both VGCNF and the growing hyperbranched macromolecules. We shall address this counterintuititive result after we have presented the solution characterization data to rule out the presence of cross-linked materials in the isolated (HBP-PEK)-*g*-VGCNF materials.

IR Spectroscopy. The IR spectra of VGCNF, HBP-PEK, and (HBP-PEK)-*g*-VGCNF are shown in Figure 1. The IR spectra of HBP-PEK and (HBP-PEK)-*g*-VGCNF are practically identical with respect to a peak-to-peak comparison. There are two types of carbonyl absorptions, i.e., the keto carbonyl band at 1659 cm^{-1} and the carboxylic acid carbonyl band at higher wavenumber, 1720 cm^{-1}, in both HBP-PEK and (HBP-PEK)-*g*-VGCNF. The broad peak from 2500 to 3500 cm^{-1} is attributed to the O−H stretch of the carboxylic acid group. Upon condensation with *o*-aminothiophenol in a PPA/P_2O_5 medium, the carboxylic acid group was converted to benzothiazole as indicated by the disappearance of the broad OH band associated with COOH absorption at 2500–3500 cm^{-1} and the carboxylic acid carbonyl band at 1720 cm^{-1}, together with the concomitant appearance of the benzothiazole band at 1604 cm^{-1} (Figure 2b). Figure 2c shows the IR spectrum of the dodecyl derivative, where the new bands at 2925 and 2854 cm^{-1} are assigned to C−H vibration of methylene groups. The carbonyl absorption is also shifted from 1720 cm^{-1} (carboxylic *C*═O) to 1723 cm^{-1} (carboxylic ester *C*═O). In MSA, it is believed that the reactive acylium intermediate derived from the carboxylic acid reacted with HN_3 to form the corresponding protonated acyl azide, which rearranged intramolecularly to form a protonated isocyanate. Upon acidic hydrolysis workup, the isocyanate was converted to the resulting amine with the concomitant expulsion of CO_2.[22] The disappearance of the *C*═O band at 1720 cm^{-1} and the appearance of a weak NH_2 stretch at 3384 cm^{-1} provide evidence of the Schmidt reaction (Figure 2d). The amine absorption is weak because of its overlap with the magnified "moisture band" in the KBr pellet around 3200–3400 cm^{-1}, stemming from the water molecules trapped in the KBr crystal lattices, despite prolonged drying at 120 °C in an oven.

Solubility. The (HBP-PEK)-*g*-VGCNF nanocomposites containing 1–40 wt % VGCNF were not soluble in nonpolar solvents, such as dichlorobenzene or toluene, but were soluble in aprotic polar solvents such as NMP and DMAc. For example, 10 wt % (HBP-PEK)-*g*-VGCNF (**3e**) could be dissolved in NMP up to 5 wt % to form stable solutions. It was only slightly soluble in ethanol but easily soluble in an ethanol/triethylamine (4:1, v/v) mixture (see Figure SI-1 in the Supporting Information and the graphical TOC). However, all (HBP-PEK)-*g*-VGCNF samples were readily dissolved in a 10% NH_4OH(aq) solution because of the ionization of the numerous surface CO_2H groups. Figure 3 shows that a red beam from a laser pointer can pass easily through 1 and 2 wt % of **3e** dissolved in a 10% NH_4OH(aq) solution but only partially through a 5 wt % solution. After months of standing under room conditions, all of the resulting solutions remained visually unchanged, i.e. appeared to be homogeneous and optically transparent-to-translucent. On the other hand, the as-received VGCNF (10 wt %) in the blend sample **7** was easily separated out because it precipitated from all of the solvents for HBP-PEK except MSA shortly after mixing. As expected, the solubility of (HBP-PEK)-*g*-VGCNF was much improved in comparison with their linear *m*PEK-based counterparts, whose

(21) PPA was used in the following cited work: Stockel, R. F.; Hall, D. M. *Nature* **1963**, *197*, 787.

(22) Vogler, E. A.; Hayes, J. M. *J. Org. Chem.* **1979**, *44* (21), 3682.

Scheme 2. Proposed Hyperbranching Polymerization of A_2B Monomers

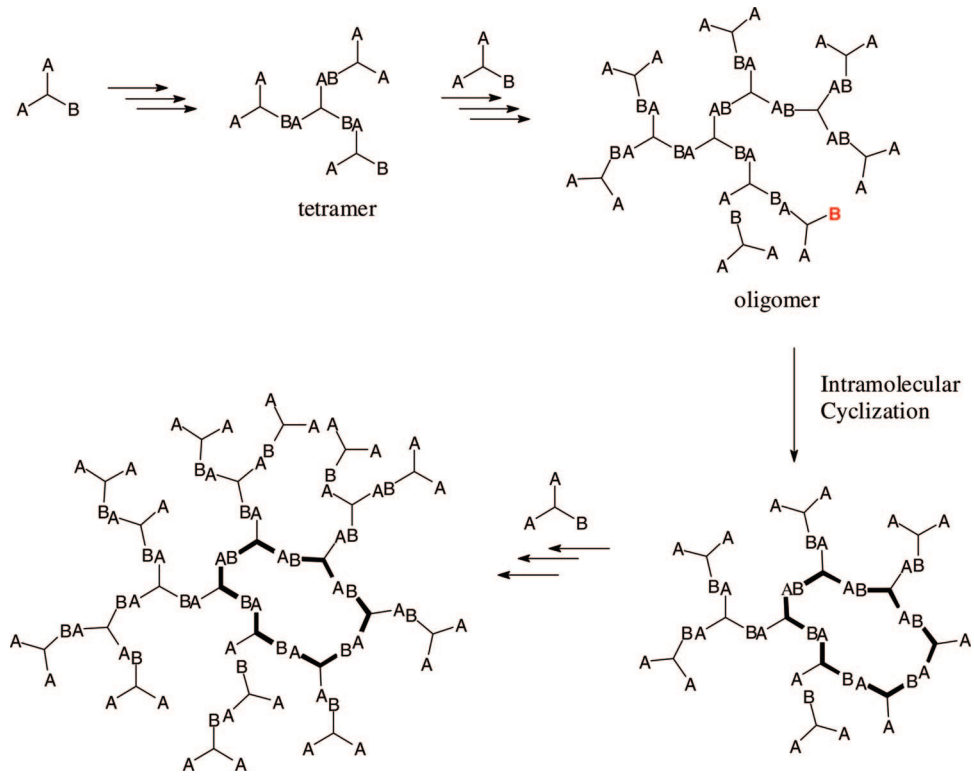

Scheme 3. Proposed Graft Polymerization of A_2B Monomers from the VGCNF Surface

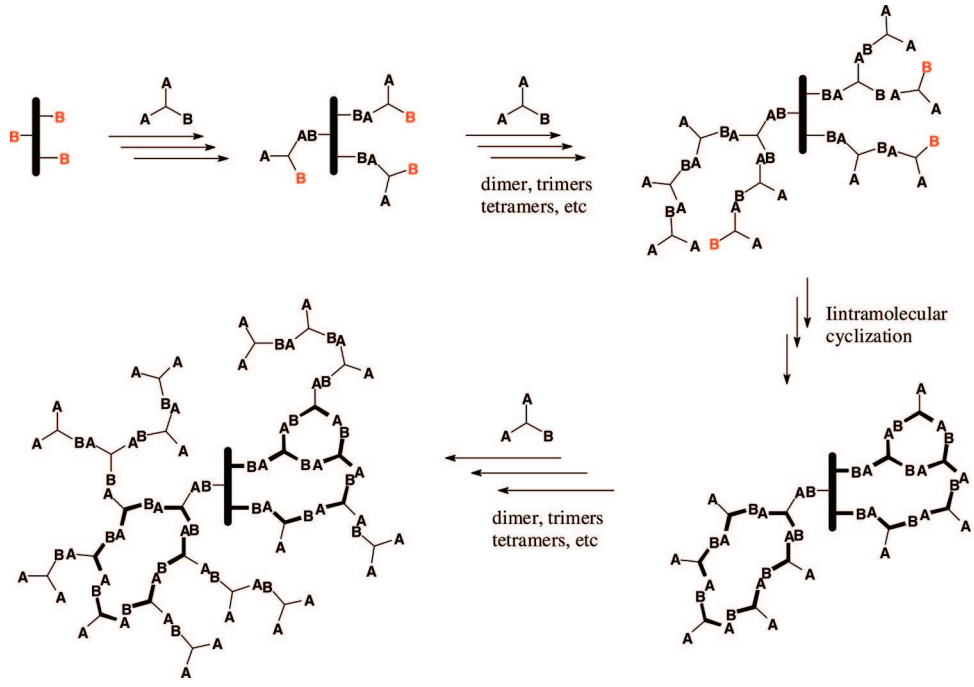

practical solubility to allow film-casting was limited only in a strongly acidic solvent such as MSA.[10b]

The organosolubility of these (HBP-PEK)-*g*-VGCNF materials could be further manipulated by simple chain-end modification with appropriate end-capping agents. In this way, the benzothiazole-terminated (HBP-PEK)-*g*-VGCNF (**4**) was soluble not only in polar solvents but also in nonpolar solvents, such as dichlorobenzene and toluene, because the benzothiazole groups are aprotic and less polar than the carboxylic acid groups. Furthermore, when the chain ends were transformed into the dodecyl ester groups, the solubility of **5** changed dramatically, and it could only be dissolved in chlorinated solvents. The solubility in these solvents is promoted by the highly nonpolar, long alkyl chains. The amine-terminated (HBP-PEK)-*g*-VGCNF (**6**) showed solubility similar to that of **3**, and they were all soluble in amide-type solvents, such as NMP and DMAc. The qualitative solubility test results are summarized in Table 1.

Intrinsic Viscosity Evaluation. Because both HBP-PEK and (HPB-PEK)-*g*-VGCNF were soluble in aprotic solvents,

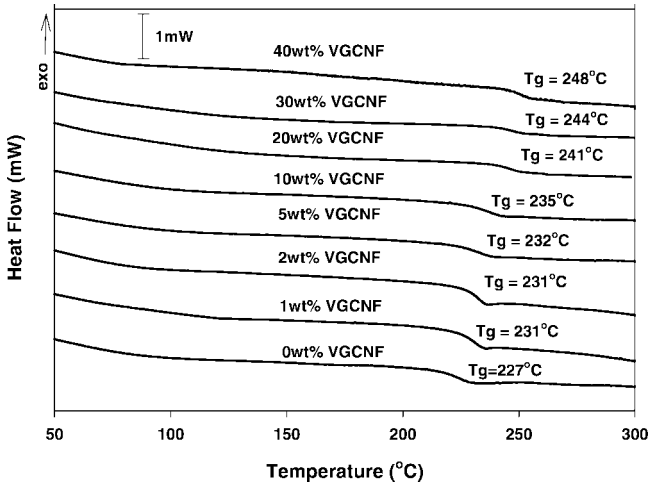

Figure 7. DSC thermograms of (HBP-PEK)-*g*-VGCNF samples scanned with a heating rate of 10 °C/min.

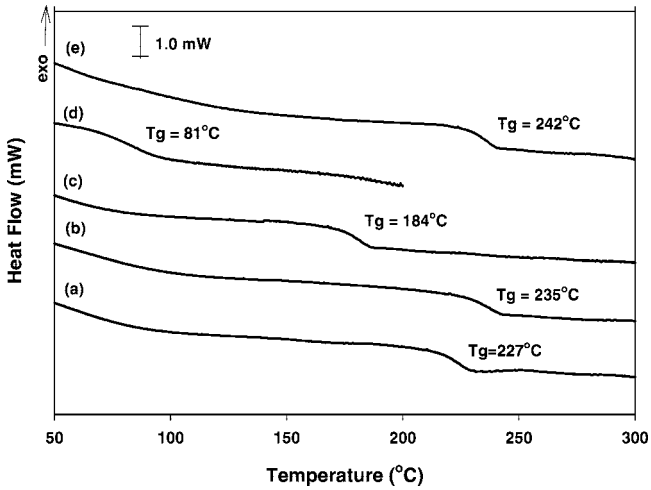

Figure 8. DSC thermograms of different end-capping (HPB-PEK)-*g*-VGCNF samples scanned with a heating rate of 10 °C/min: (a) carboxylic acid terminated HPB-PEK, 0 wt % of VGCNF; (b) carboxylic acid terminated, 10.3 wt % of VGCNF, **6e**; (c) benzothiazole-terminated, 8.2 wt % of VGCNF, **4**; (d) dodecyl-terminated, 6.9 wt % of VGCNF, **5**; (e) amine-terminated, 10.6 wt % of VGCNF,

their intrinsic viscosities were determined in NMP. After their NMP solutions had been filtered through glass filters (with practically no residue left behind), the filtrates were used to measure the reduced and inherent viscosities. Lithium bromide was used to suppress the polyelectrolyte effect stemming from the carboxylic acid groups. Both inherent and reduced viscosity data were plotted as a function of the solution concentration. As shown in Figure 4, no polyelectrolyte effect was observed, and all of the solution samples behave in a manner similar to the linear behavior of a polymer solution upon dilution. The intrinsic viscosity values were determined from the extrapolation of reduced and inherent viscosities to zero concentration (Table 1).

The $[\eta]$ of the separately synthesized HPB-PEK was 0.34 dL/g at 30 °C. In the case of the (HBP-PEK)-*g*-VGCNF, their $[\eta]$ values increased as the amount of VGCNF increased (or as the HBP-PEK content and degree of polymerization of each polymer graft decreased), from 0.41 dL/g for 1 wt % (HBP-PEK)-*g*-VGCNF to 4.89 dL/g for 40 wt % (HBP-PEK)-*g*-VGCNF. In addition, there is an apparent divergent point at around 25–27 wt % VGCNF where an accelerated rise in the intrinsic viscosity trend of (HBP-PEK)-*g*-VGCNF is observed (Figure 5). Our rationale for this observation is that, at this divergent point, the rodlike effect of VGCNF in the "hairy" (HBP-PEK)-*g*-VGCNF with increasingly shorter/smaller HPB-PEK grafts is beginning to dominate the hydrodynamic volume.

The intrinsic viscosities of chain-end-modified, 10 wt % (HBP-PEK)-*g*-VGCNF, viz., benzothiazole-terminated (**4**), dodecyl-terminated (**5**), and amine-terminated (**6**), are 0.64, 0.56, and 0.67 dL/g, respectively, which are lower than the parent (HBP-PEK)-*g*-VGCNF (CO_2H-terminated, **3e**). Intermolecular hydrogen bonding among the CO_2H end groups in **3e** is most likely the explanation for the observed higher intrinsic viscosity.

NMR. The greatly improved solubility of (HBP-PEK)-*g*-VGCNF nanocomposites in organic solvents provides a rare opportunity for solution NMR studies of polymer-modified carbon-based nanomaterials with larger diameters. While there are a number of reports for the solution NMR studies/spectra of SWNT and MWNT,[23] to our knowledge, none have been reported for chemically modified VGCNF. The solution-phase ^{1}H NMR spectra of 10 wt % (HBP-PEK)-*g*-VGCNF in DMSO-d_6 are compared with pristine HBP-PEK and the blend of HBP-PEK and VGCNF in Figure 6. Except for being broader (as is commonly observed in the NMR characterization of solubilized CNTs[23]), the aromatic proton peaks in (HBP-PEK)-*g*-VGCNF are generally similar to those in free HBP-PEK. For the VGCNF-attached PEK, the proton signals are much broader, as is commonly observed in the NMR characterization of solubilized CNTs.[23] The considerable signal broadening for HPB-PEK upon functionalization to VGCNF could, in principle, be explained in terms of two different mechanisms: a slower reorientation in solution from the attachment of HBP-PEK to nanofibers or to relaxation attributable to paramagnetic impurities in the solution. The latter is obviously relevant to the VGCNF-containing samples because the metal catalysts used for VGCNF synthesis contain paramagnetics. The as-received VGCNF used in this experiment had been heat-treated to remove carbonaceous impurities, and its reported iron content is less than 100 ppm.[4] In addition, there is some evidence that PPA was quite effective in removing the metal impurity during the reaction.[24] We have measured the proton spin–lattice (T_1) and spin–spin (T_2) relaxation times to determine if residual paramagnetic impurities make a significant contribution to the line widths for the grafted CNFs. Paramagnetic impurities greatly increase both the T_1's and T_2's and can therefore

(23) (a) Wang, X.; Liu, H.; Jin, Y.; Chen, C. *J. Phys. Chem. B* **2006**, *110*, 10236. (b) Hill, D.; Lin, Y.; Qu, L.; Kitaygorodskiy, A.; Connell, J. W.; Allard, L. F.; Sun, Y.-P. *Macromolecules* **2005**, *38*, 7670. (c) Holzinger, M.; Abraham, J.; Whelan, P.; Graupner, R.; Ley, L.; Hennrich, F.; Kappes, M.; Hirsch, A. *J. Am. Chem. Soc.* **2003**, *125*, 8566. (d) Lin, Y.; Rao, A. M.; Sadanadan, B.; Kenik, E. A.; Sun, Y.-P. *J. Phys. Chem. B* **2002**, *106*, 1294. (e) Holzinger, M.; Vostrowsky, O.; Hirsch, A.; Hennrich, F.; Kappes, M.; Weiss, R.; Jellen, F. *Angew. Chem., Int. Ed.* **2001**, *40*, 4002–4005. (f) Sun, Y.-P.; Huang, W.; Lin, Y.; Fu, K.; Kitaygorodskiy, A.; Riddle, L. A.; Yu, Y. J.; Carroll, D. L. *Chem. Mater.* **2001**, *13*, 2864.

(24) We had observed that, besides VGCNF, several MWNT samples containing metal contaminants such as iron showed considerably lower residue in TGA experiments after PPA treatment, indicating that most of the metal contaminants had been removed after this treatment.

Table 3. Thermal Properties of (HBP-PEK)-*g*-VGCNF Materials

	calcd composition[a]			TGA			
				in nitrogen		in air	
sample	VGCNF (wt %)	HBP-PEK (wt %)	DSC T_g[b] (°C)	$T_{5\%}$[c] (°C)	char at 650 °C (wt %)	$T_{5\%}$[c] (°C)	char at 650 °C (wt %)
1	100	0		>900	99.7	723	99.8
3a	0	100	227	408	55.5	387	0.7
3b	1.1	98.9	231	417	56.2	383	1.4
3c	2.2	97.8	231	417	57.7	400	2.6
3d	5.4	94.8	232	386	65.3	379	5.2
3e	10.7	89.3	235	420	61.2	410	11.0
3f	21.2	77.9	241	426	66.8	419	22.1
3g	31.5	68.5	244	414	71.2	413	31.2
3h	41.8	58.2	248	405	75.5	412	42.1
4	7.9	92.1	184	429	63.0	432	8.2
5	6.9	93.1	81	377	54.8	356	6.9
6	11.8	88.2	242	398	65.8	394	10.6
7	10.7	89.3	227	414	60.4	402	10.2

[a] Calculation based on the assumption that VGCNF is 100% C and the molar mass of the repeat unit of HBP-PEK is 240.22. [b] Inflection in the baseline on the DSC thermogram obtained in N_2 with a heating rate of 10 °C/min. [c] Temperature at which 5% weight loss occurred on the TGA thermogram obtained with a heating rate of 10 °C/min.

affect the line width. The polymers grafted to CNFs are slowly tumbling macromolecules and are expected to have long (seconds) relaxation times, so any paramagnetic contribution should be easily detected. The proton T_1's measured by inversion–recovery for the 10 wt % (HBP-PEK)-*g*-VGCNF in DMSO-d_6 were 3.93 and 6.81 s for the peaks at 7.8 and 7.1 ppm, respectively. These long T_1's rule out any significant contribution from paramagnetic impurities. In addion, we measured the spectrum for the 10 wt % HBP-PEK/VGCNF blend dispersed in deuterated DMSO by sonication. The mixture showed good dispersion in DMSO (Figure 6, spectrum b), but the proton signals do not show the broad lines that we observe for the (HBP-PEK)-*g*-VGCNF solutions (Figure 6, spectrum c).

These results show that the broad proton signals for the grafted sample are most likely due to the high molecular weight and low mobility of HBP-PEK after it has been grafted onto VGCNF. (HBP-PEK)-*g*-VGCNFs were readily soluble in deuterated DMSO without any sonication, and its solution was stable on the bench for months. In the case of the blend, the VGCNF precipitated out from DMSO 1 week after sonication (Figure SI-2 in the Supporting Information), which further proves that VGCNF was solubilized with the aid of the covalently bonded HPB-PEK. Overall, the results provide another piece of evidence to strongly support that VGCNF has been grafted with relatively high molecular weight HPB-PEK.

Explanation for the Absence of Gelation and Cross-Linking. The collective evidence from (i) solubility tests in various organic, aqueous, and strongly acidic solvents, (ii) viscosity experiments, and (iii) NMR relaxation time experiments has all indicated that there was an absence of gels or cross-linked materials in the Soxhlet-extracted (HBP-PEK)-*g*-VGCNF samples. A plausible explanation is as follows. In Scheme 2, we propose an idealized polymerization process of the A_2B monomer (where A = CO_2H function and B = sp^2 C−H bond para to the ether linkage). In principle, as the degree of polymerization (n) increases in a growing hyperbranched polymer, the number of A corresponds to $n + 1$ and the number of B is always unity. However, the fate of B (focal point group) could happen as follows: it can either (i) be destroyed by intramolecular cyclization[25] via F−C acylation or (ii) be so sterically inaccessible for the F−C reaction with a A_2B molecule or intramolecular cyclization that it is "buried" deep inside the hyperbranched structure. In both scenarios, only A functions at the peripheries of the growing hyperbranched macromolecules are available for the F−C reaction until all of the A_2B monomers are consumed. In Scheme 3, the encounter of AB_2 molecules and unfunctionalized VGCNF (where B is sp^2 C−H at the defect sites) should lead quickly to the growth of hyperbranched grafts, where the number of A is defined by the degree of polymerization (n) and B is invariably unity. It is postulated that the intramolecular cyclization would have occurred at the degrees of polymerization lower than that for the polymerization of AB_2 monomers to form the unattached hyperbranched macromolecules based on the rationale that the restriction imposed on both the mobility and the space for each hyperbranched graft to move around the surface area of VGCNF can actually increase the probability of A to react with B intramolecularly. The resulting entity now with only peripheral A's can continue to grow with either the remaining AB_2 monomers or free hyperbranched oligomers (each with a single B focal point group).

It should be pointed out that while this hypothesis reasonably accounts for the absence of cross-linking and the lack of gel formation in this system, it does not rule out completely the nonexistence of free HPB-PEK. On the basis of the results from extraction experiments in this work, we estimate that its content is 5–7 wt % as the upper limit for this system.

Thermal Properties. The glass transition (T_g) temperatures were determined by DSC by heating to 300 °C in a DSC chamber and cooling to 25 °C under a nitrogen purge

(25) (i) Intramolecular cyclization in the synthesis of various types of hyperbranched polymers are well documented. Himmelberg, P.; Fossum, E. *J. Polym. Sci., Part A: Polym. Chem.* **2005**, *43*, 3178. (ii) Baek, J.-B.; Harris, F. W. *Macromolecules* **2005**, *38*, 297. (iii) Galina, H.; Lechowicz, J. B.; Walczak, M. *Macromolecules* **2002**, *35*, 3253. (iv) Simon, P. F. W.; Mueller, A. H. E. *Macromolecules* **2001**, *34*, 6206. (v) Gong, C.; Miravet, J.; Frechet, J. M. J. *J. Polym. Sci., Part A: Polym. Chem.* **1999**, *37*, 3193. (vi) Chu, F.; Hawker, C. J.; Pomery, P. J.; Hill, D. J. T. *J. Polym. Sci., Part A: Polym. Chem.* **1997**, *35*, 1627.

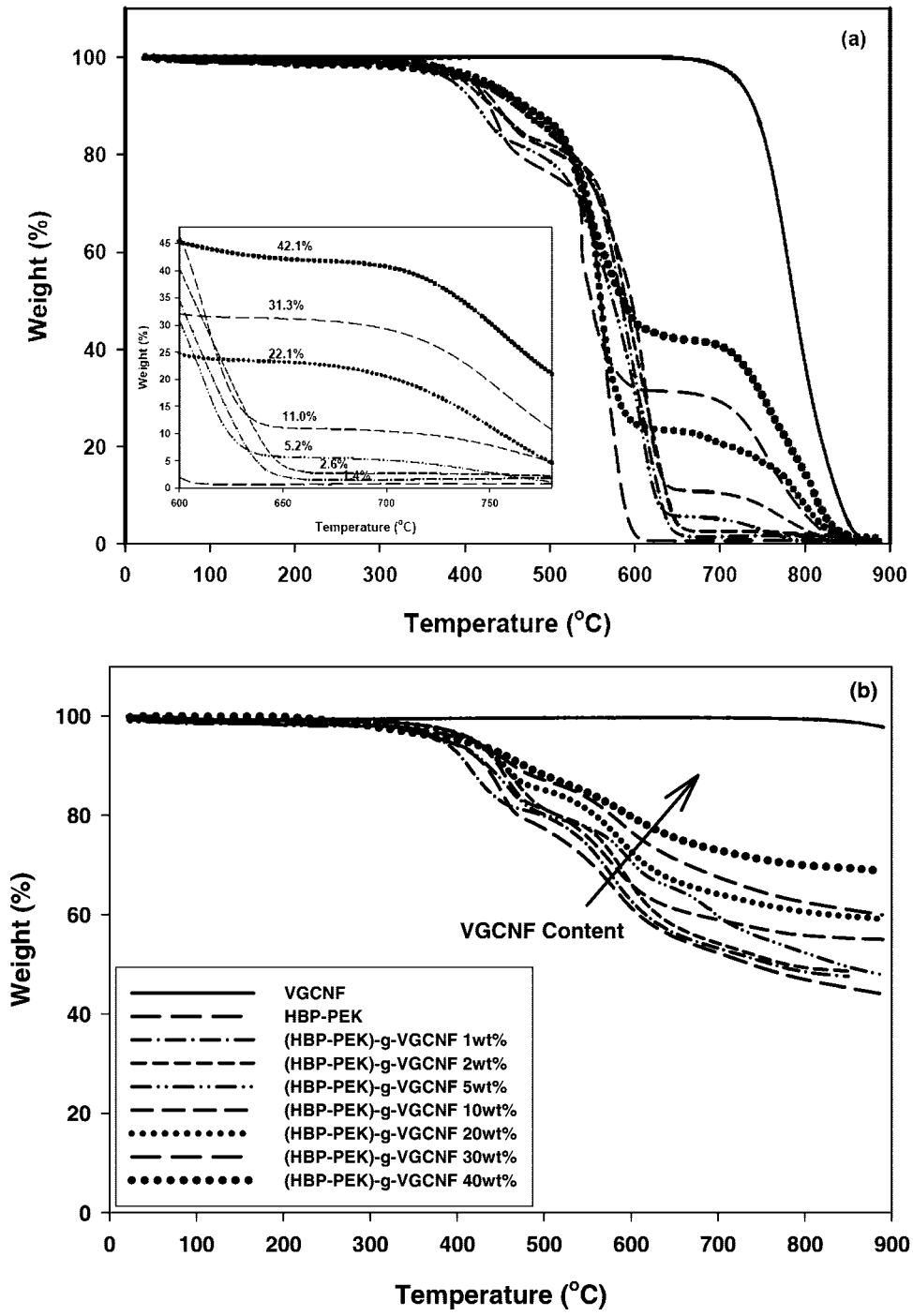

Figure 9. TGA thermograms of (HBP-PEK)-*g*-VGCNF samples scanned with a heating rate of 10 °C/min (a) in air and (b) in nitrogen.

to eliminate the thermal history effects. The samples were then heated to 300 °C again, and T_g values were taken as the midpoint of the maximum baseline shift from the second heating run. The hyperbranched homopolymer, HBP-PEK, exhibited a T_g of 227 °C, and the same T_g value was observed for a physical blend containing 10 wt % of as-received VGCNF. In the cases of in situ synthesized (HBP-PEK)-*g*-VGCNF materials, a single T_g was observed for all samples. In addition, when the VGCNF amount was increased, their T_g's were monotonously increased from 227 to 248 °C for 40 wt % (HBP-PEK)-*g*-VGCNF (Figure 7). In our previous work, when linear *m*PEK was grafted to VGCNF, similar results were also obtained.[10b] Because the flexible polymer chains were attached to the rigid VGCNF surface, its mobility was constrained, and the T_g's had increased as much as 21 °C.

After **3e** (T_g = 235 °C) had been end-capped with a benzothiazole functionality, the T_g of the derivative **4** decreased to 184 °C. The T_g of the dodecyl-terminated (HBP-PEK)-*g*-VGCNF (**5**) was further lowered to 81 °C because the nonpolar dodecyl chains could also act as an internal plasticizer outside the polymer's periphery, which had reduced the glass transition temperature as much as 154 °C. The amine-terminated (HBP-PEK)-*g*-VGCNF contained about 10 wt % of VGCNF. Its T_g of 242 °C was similar to the carboxylic acid terminated analogue (Figure 8and Table 3).

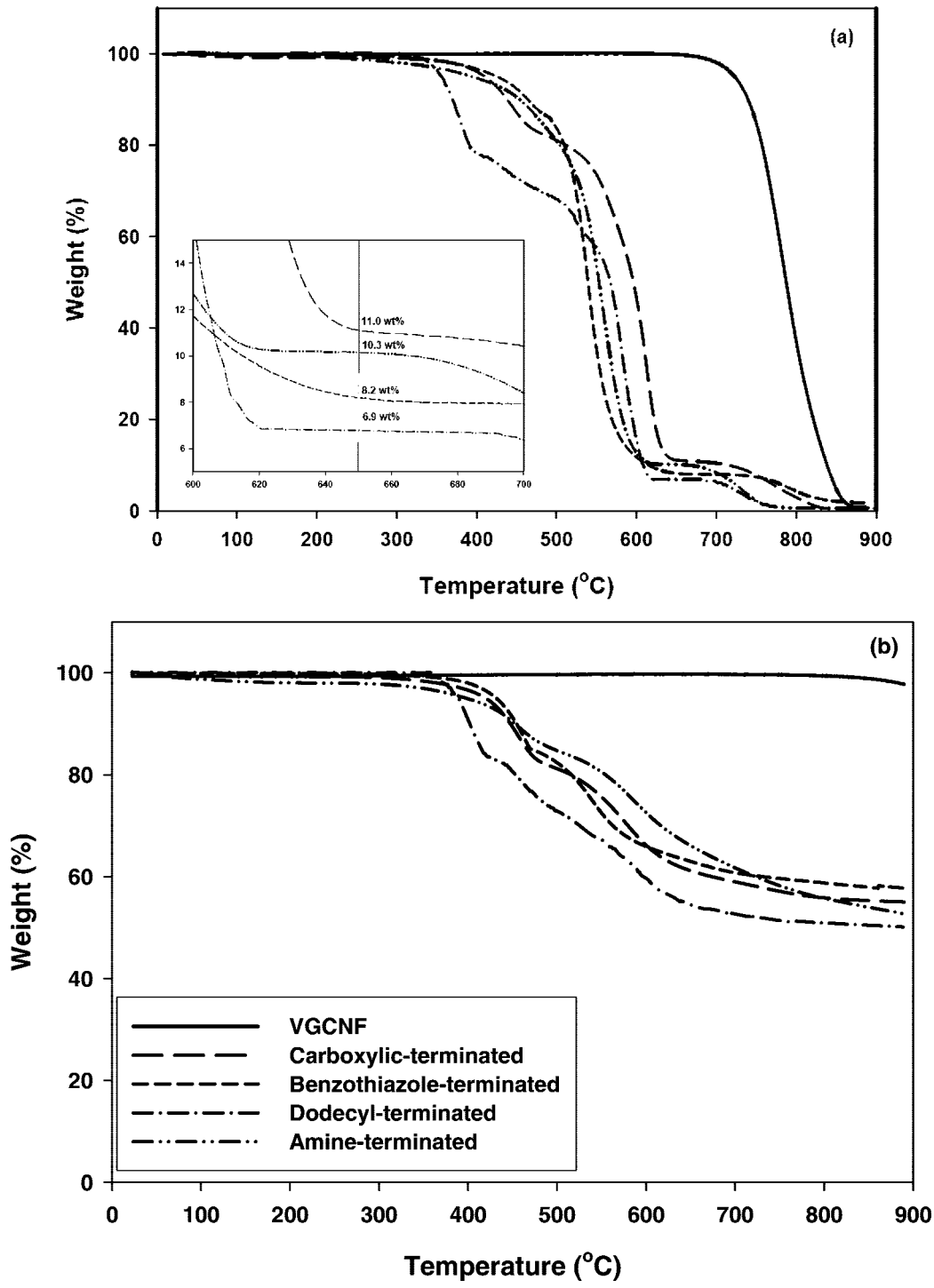

Figure 10. TGA thermograms of end-capped (HBP-PEK)-*g*-VGCNF samples scanned with a heating rate of 10 °C/min (a) in air and (b) in nitrogen.

As we have shown previously,[10] the combination of a model reaction, TGA experiments, and elemental analysis is a simple, yet powerful method to quantify the degree of functionalization as well as the VGCNF and PEK compositions in the resulting materials. The pristine VGCNF exhibited an expectedly high thermal stability, with 5 wt % weight loss ($T_{d5\%}$) occurring at 723 °C in air and at temperatures higher than 900 °C in nitrogen. HBP-PEK and (HBP-PEK)-*g*-VGCNF displayed $T_{d5\%}$ in the range of 486–426 °C in air and 379–420 °C in nitrogen, respectively (Figure 9). The char yield at 650 °C in air, after HBP-PEK had been thermooxidatively stripped off, was used to determine the original amount of VGCNF. Excellent agreement was obtained between the theoretical and experimental values for all of the HBP-PEK/VGCNF compositions (Table 2).

TGA results for the chain-end-modified (HBP-PEK)-*g*-VGCNF materials (**4**−**6**) are shown in Figure 10 and Table 3. Benzothiazole-terminated (HBP-PEK)-*g*-VGCNF exhibited the highest $T_{d5\%}$ (429 °C in air and 432 °C in nitrogen) because the benzothiazole group is most thermally and thermooxidatively stable among the end-group functionalities used in this work. The thermal stability of **5** was the lowest because its alkyl end groups. The amine-terminated (HBP-

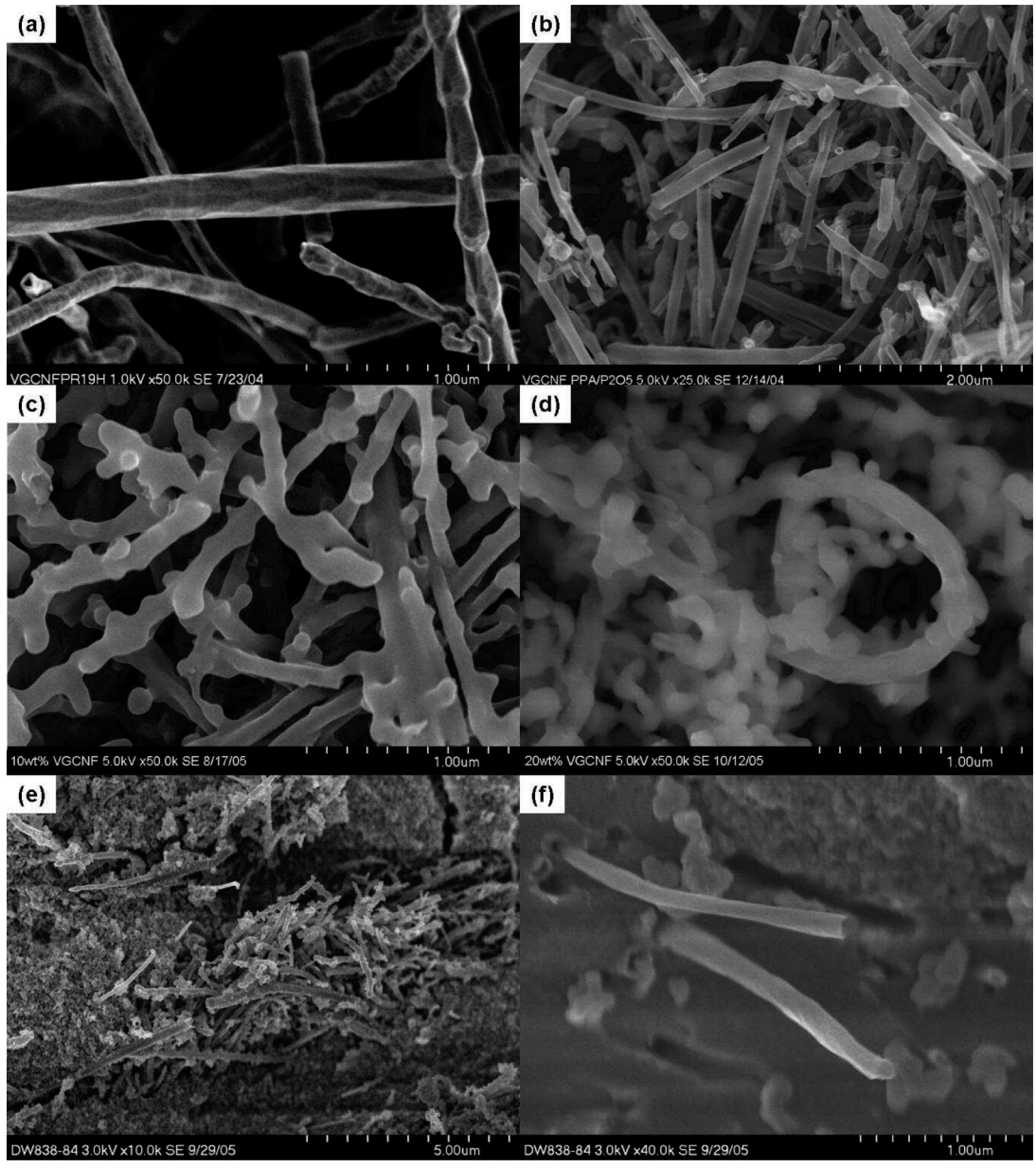

Figure 11. SEM images of (a) pristine VGCNF (×50K), (b) PPA/P_2O_5 treated VGCNF (×25K), (c) 10 wt % (HBP-PEK)-*g*-VGCNF (×50K), (d) 20 wt % (HBP-PEK)-*g*-VGCNF (×50K), (e) 10 wt % (HBP-PEK)/VGCNF blend (×10K), and (f) 10 wt % (HBP-PEK)/VGCNF blend (×40K).

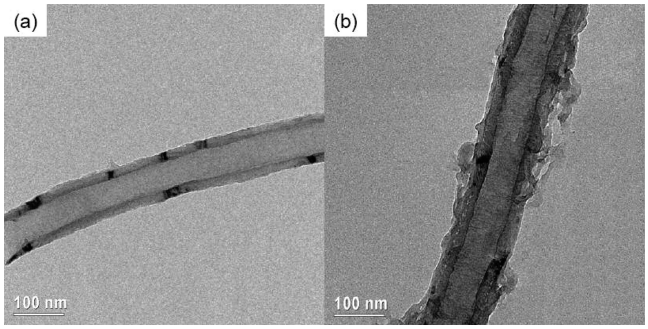

Figure 12. TEM images of (HBP-PEK)-*g*-VGCNF: (a) pristine VGCNF; (b) 20 wt % (HBP-PEK)-*g*-VGCNF.

PEK)-*g*-VGCNF (**6**) shows thermal stability similar to that of **3**. After chain-end modification of the 10 wt % HBP-PEK)-*g*-VGCNF had been accomplished with benzothiazole, alkyl, and amine groups, the theoretical VGCNF contents were changed accordingly to 7.9, 6.9, and 11.8 wt %, respectively. The char yields of **4**−**6** at 650 °C are 8.2, 6.9, and 10.3 wt %, which agree well with the respective theoretical values (Table 2).

Scanning Electron Microscopy (SEM). The SEM image of pristine VGCNF shows that most of the tube surfaces are clean, as shown in Figure 11a. Some of the nanotube surfaces display "stacked Dixie cups" or bamboo texture, and the average diameter is in the range of 100–200 nm. In order to investigate the effect of PPA/P_2O_5 on VGCNF, a control experiment was run where VGCNF without TMPBA was heated in PPA/P_2O_5 at 130 °C for 3 days to afford a PPA-treated sample (PT-VGCNF) in 94% recovery yield. The workup was the same as that for (HPB-PEK)-*g*-VGCNF. PT-VGCNF has slightly lower carbon and hydrogen contents than pristine VGCNF, although the differences are in the range of experimental errors. The pristine and PPA-treated VGCNF share the same morphologies including surface,

diameter, and length, as shown in Figure 11b. This confirms that PPA/P_2O_5 is indeed a mild, nondestructive medium for F−C reactions on carbon nanosurfaces. The surfaces of 10 and 20 wt % (HBP-PEK)-*g*-VGCNF are highly coated with the polymer ,and the original VGCNF texture such as stacked Dixie cups was lost as a result of the polymer grafting, as shown in parts c and d of Figure 11. The average diameters of (HBP-PEK)-*g*-VGCNF increased slightly. The morphology of a 10 wt % VGCNF/HBP-PEK physical blend, **7**, was also investigated using SEM. The elemental analysis results of **7** and **3e** are similar (Table 1), indicative of both containing similar components. However, large clusters of aggregated VGCNF were observed under SEM, as shown in Figure 11e. Furthermore, the VGCNF surface, as shown in Figure 11f, was obviously clean without any tethered polymer, which confirmed that **7** was indeed a physical blend.

TEM. The TEM image of pristine VGCNF shows that the nanofiber surface is smooth (Figure 12). However, the nanofiber surfaces of 20 wt % (HBP-PEK)-*g*-VGCNF are rough and fuzzy, and there is an obvious increase in the diameter as well. We attribute this diameter increase to the heavy coating by the HPB-PEK (thickness of approximately 10–20 nm).

Conclusion

Our results show that (HBP-PEK)-*g*-VGCNFs have considerably better solubility (e.g., in aprotic polar solvents) than their linear analogues, *m*PEK-*g*-VGCNF, validating our concept in using an aromatic hyperbranched structure to enhance the organosolubility and widen the processing options of CNF/CNT materials. In our in situ hyperbranching polycondenation process, despite the multifunctionality existing in each reacting species, it is noteworthy that no gelation stemming from potential cross-linking reactions was observed for all of the in situ synthesis experiments conducted. While many efforts to solubilize smaller and shorter carbon-based one-dimensional nanomaterials have been reported in the literature, our results confirm the feasibility of solubilization for much wider and extremely long nanotubes.[26] Furthermore, because of the greatly reduced viscosity for hyperbranched polymers, (HBP-PEK)-*g*-VGCNF would be amenable to applications where speed and large-area coverage are required, such as spraying and painting techniques. In addition, we also show that the overall polarity of (HBP-PEK)-*g*-VGCNF can be synthetically controlled by converting the terminal CO_2H groups of the HBP-PEK grafts to amine, benzothiazole, and dodecyl ester groups. The former two cases could be conducted in a one-pot fashion by the addition of the respective end-capping agents after the A_2B polymerization in PPA has completed. We have also demonstrated that polarity modification via an in situ $A_3 + B_2$ polymerization with judicious stoichiometric variation of the triacid (A_3) and bis(phenyl ether) (B_2) monomers can be used.[27] As expected, the nature of the chain ends can dramatically affect the physical properties of the resulting (HBP-PEK)-*g*-VGCNF materials. For example, the dodecyl-terminated (HBP-PEK)-*g*-VGCNF displayed an excellent solubility in chloroform and a much lower T_g than the CO_2H-terminated analogue. Most importantly, we have demonstrated that aromatic hyperbranched polymers (accessible only via step-growth polymerization) with its vast number of end groups and random structures can be a very useful tool in enhancing solubility, introducing application-specific functionality (e.g., lithium−hydrogen exchange for ion conductivity and battery applications),[27] and modulating thermal properties of the polymer nanocomposites with high contents of CNF/CNT materials for higher temperature applications.

Acknowledgment. We are grateful to Sharon Simko (University of Dayton Research Institute) for her assistance in the monomer synthesis and Marlene Houtz and Gary Price (both of University of Dayton Research Institute) for acquiring TGA and SEM data and images. This project was supported by funding from Wright Brother Institute (Dayton), Office of Scientific Research (AFOSR), and Materials & Manufacturing Directorate, U.S. Air Force Research Laboratory.

Supporting Information Available: Figure SI-1, which shows visually the solubility of **3e** in various solvents for (a) 0.10 wt % in NMP, (b) 1.0 wt % in NMP, (c) 5.0 wt % in NMP, (d) 1.0 wt % in DCB, (e) 1.0 wt % in ethanol, and (f) 1.0 wt % in ethanol/triethylamine, and Figure SI-2, which shows photographically DMSO-d_6 solutions of a 10 wt % VGCNF/(HBP-PEK) blend **7** and 10 wt % (HBP-PEK)-*g*-VGCNF, **3e**, (a) right after sonication, (b) for **3e** after mixing without sonication; (c) for **7** after 1 week on the bench but sedimentation had occurred overnight after mixing, and (d) for **3e** after 1 week on the bench. This material is available free of charge via the Internet at http: //pubs.acs.org.

CM702857Z

(26) (a) For recent reviews, see: Tasis, D.; Tagmatarchis, N.; Bianco, A.; Prato, M. *Chem Rev. Chem. Rev.* **2006**, *106*, 1105–1136. (b) Rakov, E. G. Chemistry of Carbon Nanotubes. In *Nanotubes and Nanofibers*; Yury, G., Ed.; CRC Press LLC: Boca Raton, FL, 2006; pp 37–107.

(27) Choi, J.-Y.; Oh, S.-J.; Lee, H.-J.; Wang, D. H,; Tan, L.-S.; Baek, J.-B. *Macromolecules* **2007**, *40*, 4474. It should be pointed out that, during the in situ $A_3 + B_2$ polycondensation, we did not observe any cross-linking reaction or gelation.